Metal/*p*-InSe:Mn Schottky Barrier Diodes

S.DUMAN*, Z. ELKOCA, B. GURBULAK, T. BAHTIYARI TEKLE, S. DOGAN
Department of Physics, Faculty of Sciences, Atatürk University, 25240, Erzurum, Turkey

In this study, we have reported a study of a number of metal/*p*-type InSe:Mn (Al, Au, Au-Be, Au-Ge, Au-Zn, Cd, Co, Mn, Sb, Sn and Zn) Schottky barrier diodes (SBDs). The barrier height (BH) and ideality factor (*n*) values for the metal/*p*-InSe:Mn SBDs have been obtained from their *I–V* characteristics at the room temperature. At high currents in the forward direction, the series resistance effect has been observed. The value of series resistance has been determined from *I–V* measurements using Cheung's functions.

(Received October 6, 2011; accepted July 19, 2012)

Keywords: Layered semiconductors; InSe; Schottky diode; Barrier height

1. Introduction

The chemical bonds in InSe semiconductor are almost complete within the layers which make the surfaces of this material free of dangling bonds and suitable for device applications [1]. Its cleaved surfaces do not required any additional treatment at *p–n* junction formation and are chemically inert at ambient conditions [2]. The only disadvantage of InSe single crystals is their high resistivity, being a cause of considerable series resistance in corresponding photovoltaic devices [2]. Because of interesting physical properties, the applications of InSe are extensive, such as for Schottky diodes [3-5] and photoconductors [6], in the fields of solar cells [7], batteries [8].

In our preivous studies, Au-Ge/*n*-InSe:Sn [3] and Au-Be/*p*-InSe:Cd [4] Schottky contacts were fabricated and their electrical characteristics were examined. In Ref. [3], an experimental BH value of about 0.70 eV was obtained for the Au–Ge/*n*-InSe:Sn Schottky diode at 300 K. From the I–V characteristics, the BH values varied between 0.74 eV and 0.82 eV with values of ideality factors ranging between 1.49 and 1.11 were obtained for the Au–Be/*p*-InSe:Cd SBDs, in Ref. [4]. For Au/InSe Schottky diode, SBH values ranging from 0.7 to 0.75 eV were deduced with ideality factors of 1.03 and 1.11, respectively [5]. In this study, Schottky contacts have been fabricated by thermal evaporation technique using several metals (Ag, Al, Au, Au-Be, Au-Ge, Au-Zn, Cd, Co, Mn, Sb, Sn, Zn) having a different metal work function to *p*-InSe:Mn. The BH and ideality factor (*n*) values for the metal/*p*-InSe:Mn SBDs have been obtained from their *I–V* characteristics at the room temperature. The series resistance effect has been observed from the forward bias region of *I–V* characteristics and these values have been determined using Cheung functions. To our knowledge, it has not yet been reported information about SBDs including various metals on *p*-InSe:Mn in the literature.

2. Experimental procedure

p-InSe:Mn monocrystal was grown in our crystal growth laboratory by using a modified Bridgman–Stockbarger method. Undoped InSe crystals always have *n*-type conductivity. Mn doped InSe crystal has *p*-type conductivitiy. The hot probe technique was used to determine the type of conductivity in the InSe:Mn semiconductor. The sample used in this work were freshly and gently cleaved with a razor blade from the grown ingots and no further polishing or cleaning treatment was required because of the natural mirror-like cleavage faces of the samples. The low-resistance ohmic contact was made by evaporating indium (In) metal on the one side of the *p*-InSe:Mn substrate in a vacuum-coating unit of 10^{-5} Torr, followed by a temperature treatment at 300°C for 3 min. in flowing N_2. The Schottky contacts (Ag, Al, Au, Au-Be, Au-Ge, Au-Zn, Cd, Co, Mn, Sb, Sn, Zn) were formed by evaporating metals as dots with diameter of about 1 mm on the other surface of the *p*-InSe:Mn. The *I–V* characteristics were measured using a Keithley 487 Picoammeter/Voltage Source at the room temperature and under dark conditions.

3. Results and discussions

The current through a uniform metal-semiconductor interface due to TE can be expressed as [9]

$$I = I_0\left[\exp\left(\frac{qV}{nkT}\right)-1\right] \quad (1)$$

where I_0 is the saturation current defined by

$$I_0 = AA^*T^2\exp\left(-\frac{q\Phi_{b0}}{kT}\right) \quad (2)$$

where, the quantities V, A, A^*, T, k, q, Φ_{b0} and n are the forward-bias voltage, the effective diode area, effective Richardson constant for *p*-type InP, temperature in Kelvin, Boltzmann constant, electronic charge and the zero bias apparent BH and ideality factor, respectively. From Eq. (1), n can be written as

$$n = \frac{q}{kT}\left(\frac{dV}{d(\ln I)}\right) \tag{3}$$

n is introduced to take the deviation of the experimental *I-V* results from the ideal thermionic model into account or to include the contributions of other current transport mechanisms. It should be n= 1 for an ideal contact.

Using the thermionic emission theory [9,10] for prepared metal/*p*-InSe:Mn SBDs, the experimental values of the SBH and the n were determined from the current axis intercept and the slope of the linear region (indicating that the effect of series resistance in this region was not important) [11] of the forward bias ln(*I–V*) characteristics, respectively. For SBDs of Ag/*p*-InSe:Mn, Al/*p*-InSe:Mn, Au/*p*-InSe:Mn, Au-Be/*p*-InSe:Mn, Au-Ge/*p*-InSe:Mn, Au-Zn/*p*-InSe:Mn, Cd/*p*-InSe:Mn, Co/*p*-InSe:Mn, Mn/*p*-InSe:Mn, Sb/*p*-InSe:Mn ,Sn/*p*-InSe:Mn and Zn/*p*-InSe:Mn, the experimental semi-log forward-and reverse-bias ln*I*–V characteristics obtained at room temperature are given Figs. 1–12, respectively. The parameters obtained for all of the metal/*p*-InSe:Mn SBDs fabricated are given in Table I. The BH and n values for the metal/*p*-InSe:Mn SBDs have varied from 0.75 to 1.01 eV, and from 1.51 to 1.15, respectively.

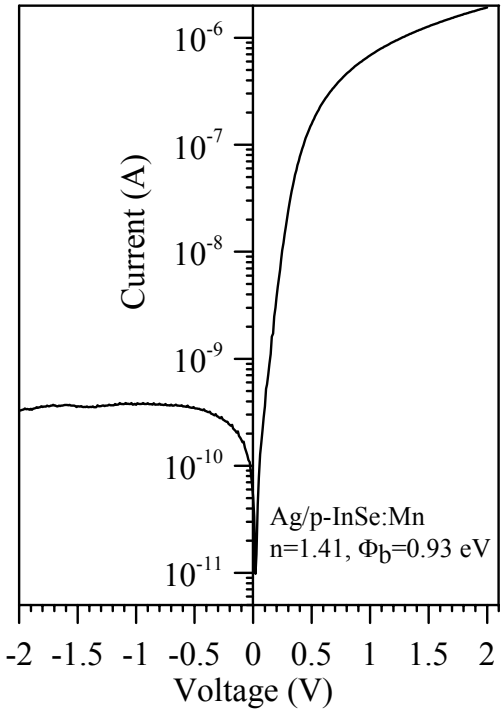

Fig. 1. Forward- and reverse-bias ln(I)–V characteristics of the Ag/p-InSe:Mn Schottky barrier diode at room temperature.

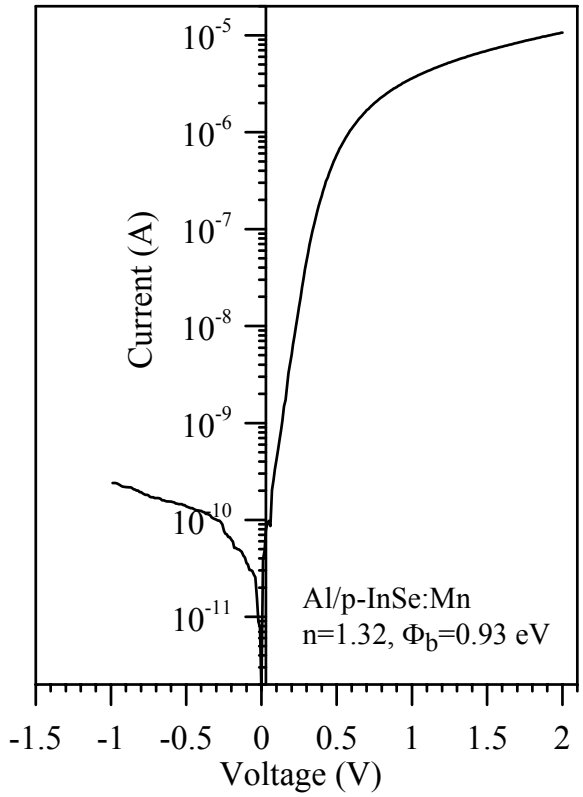

Fig. 2. Forward- and reverse-bias ln(I)–V characteristics of the Al/p-InSe:Mn Schottky barrier diode at room temperature.

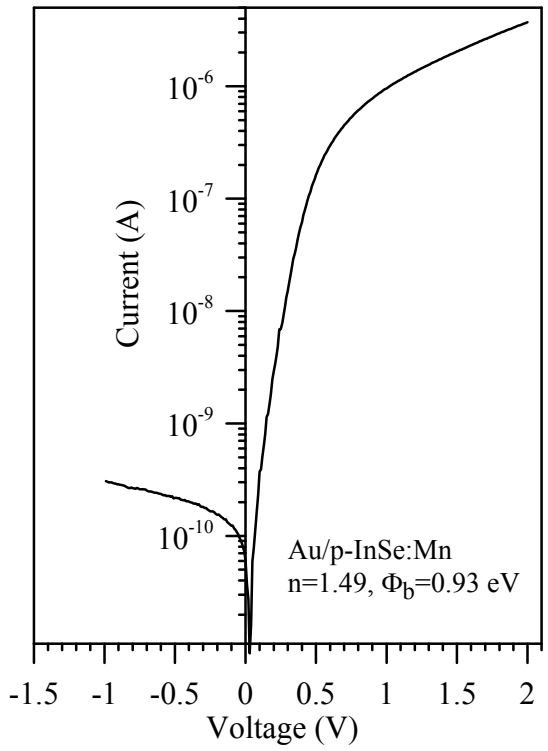

Fig. 3. Forward- and reverse-bias ln(I)–V characteristics of the Au/p-InSe:Mn Schottky barrier diode at room temperature.

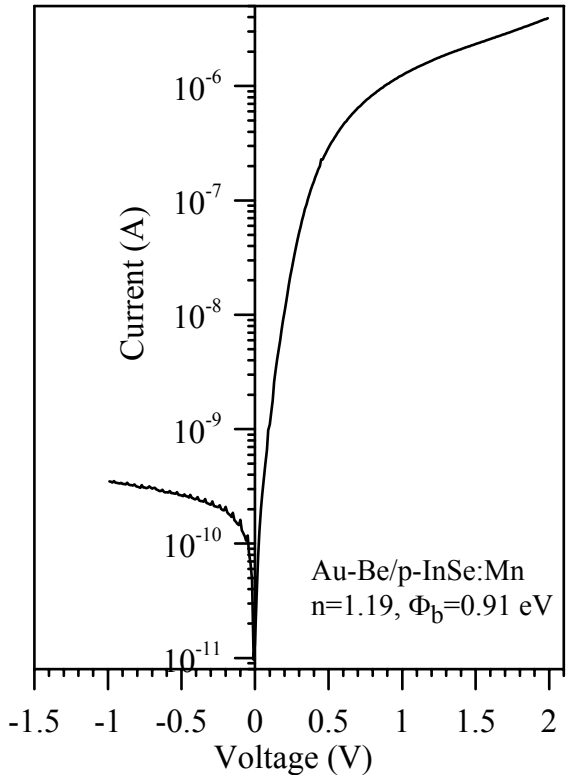

Fig. 4. Forward- and reverse-bias ln(I)–V characteristics of the Au-Be/p-InSe:Mn Schottky barrier diode at room temperature.

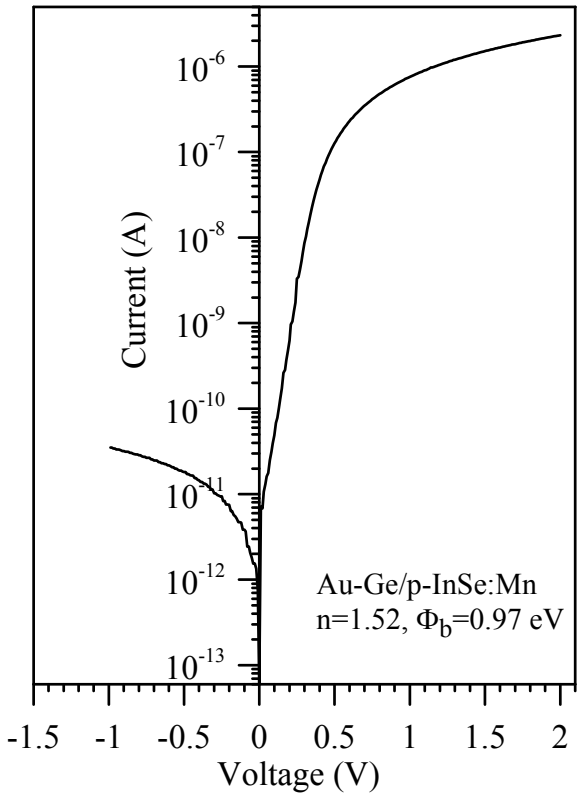

Fig. 5. Forward- and reverse-bias ln(I)–V characteristics of the Au-Ge/p-InSe:Mn Schottky barrier diode at room temperature.

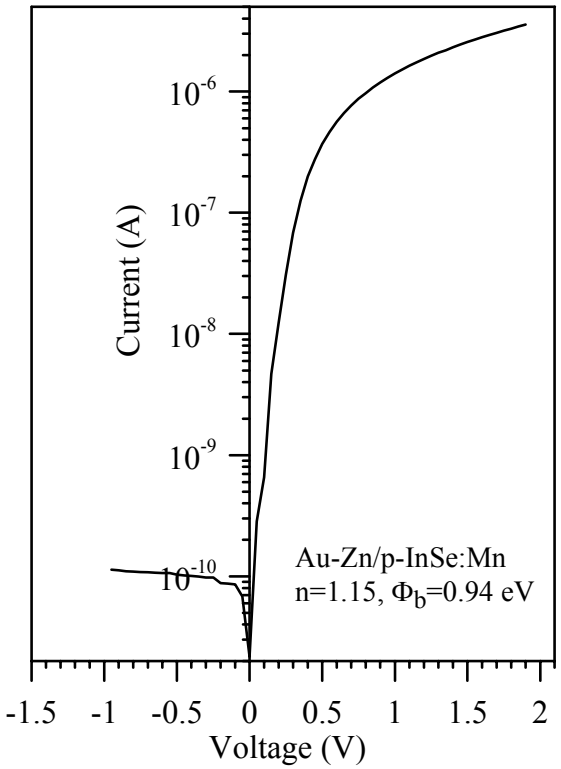

Fig. 6. Forward- and reverse-bias ln(I)–V characteristics of the Au-Zn/p-InSe:Mn Schottky barrier diode at room temperature.

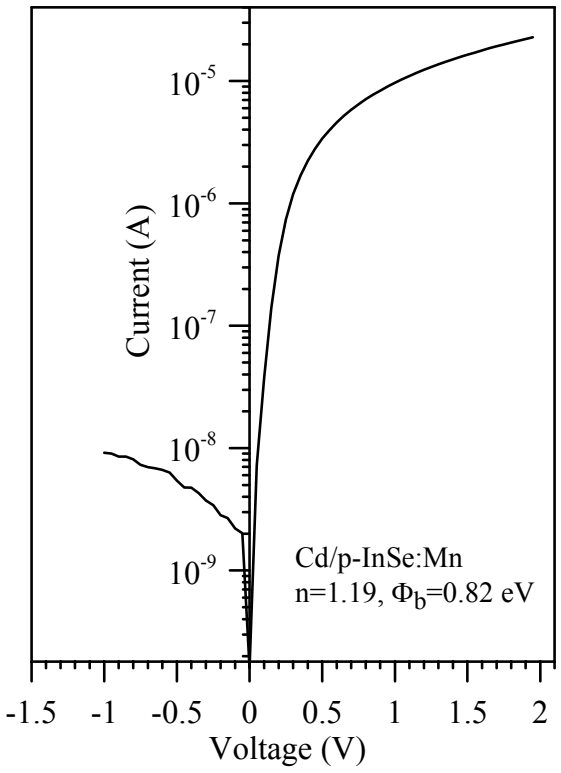

Fig. 7. Forward- and reverse-bias ln(I)–V characteristics of the Cd/p-InSe:Mn Schottky barrier diode at room temperature.

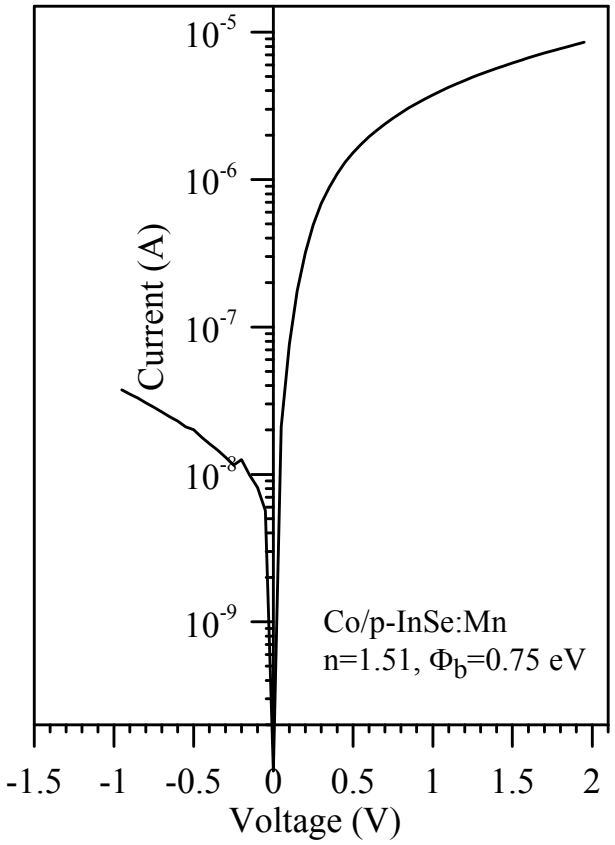

Fig. 8. Forward- and reverse-bias ln(I)–V characteristics of the Co/p-InSe:Mn Schottky barrier diode at room temperature.

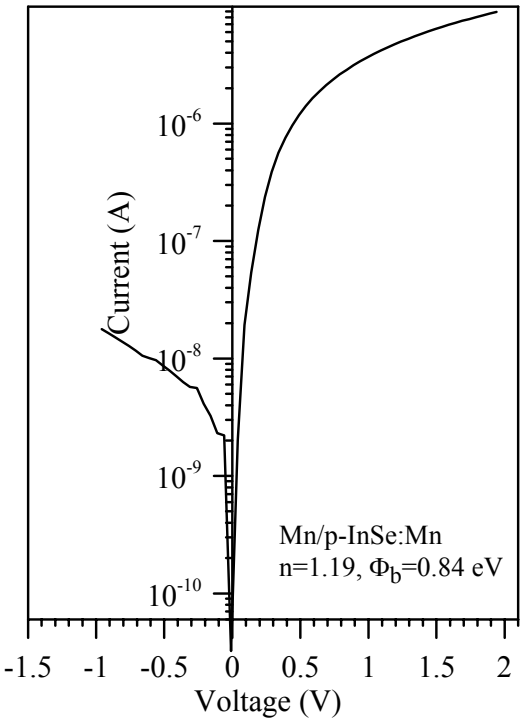

Fig. 9. Forward- and reverse-bias ln(I)–V characteristics of the Mn/p-InSe:Mn Schottky barrier diode at room temperature.

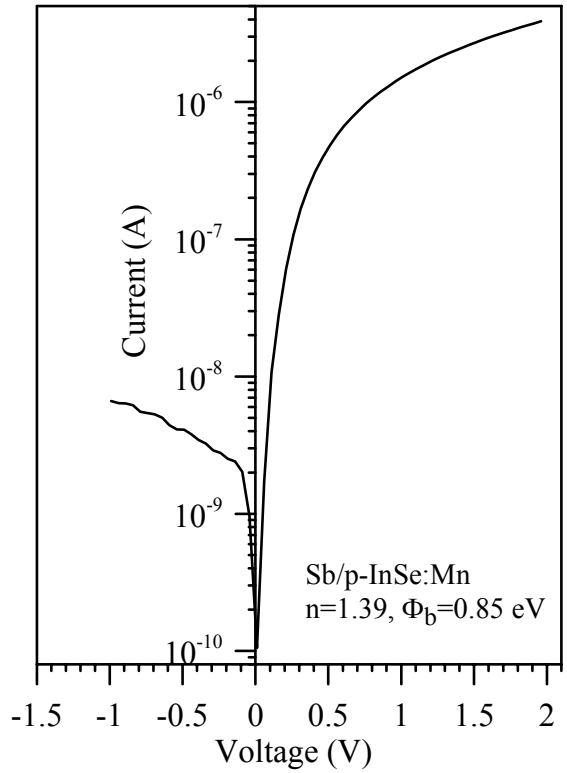

Fig. 10. Forward- and reverse-bias ln(I)–V characteristics of the Sb/p-InSe:Mn Schottky barrier diode at room temperature.

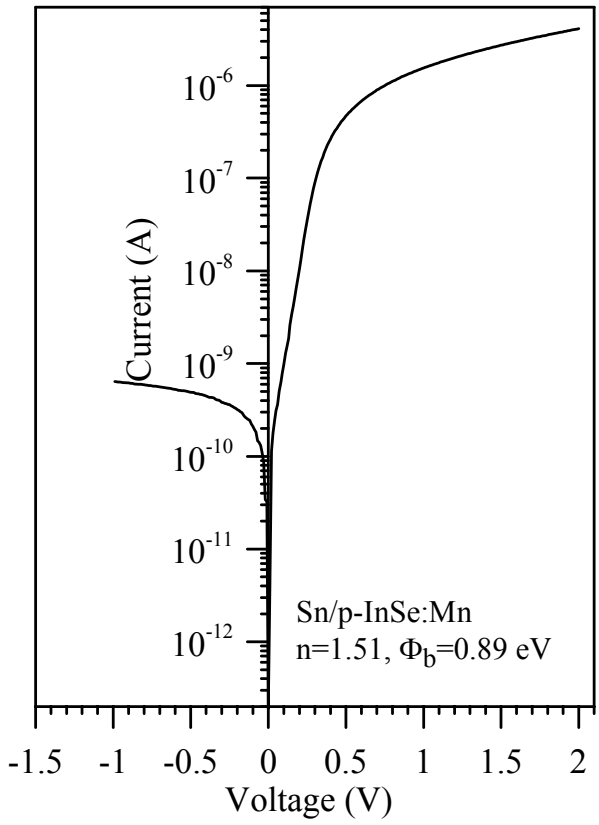

Fig. 11. Forward- and reverse-bias ln(I)–V characteristics of the Sn/p-InSe:Mn Schottky barrier diode at room temperature.

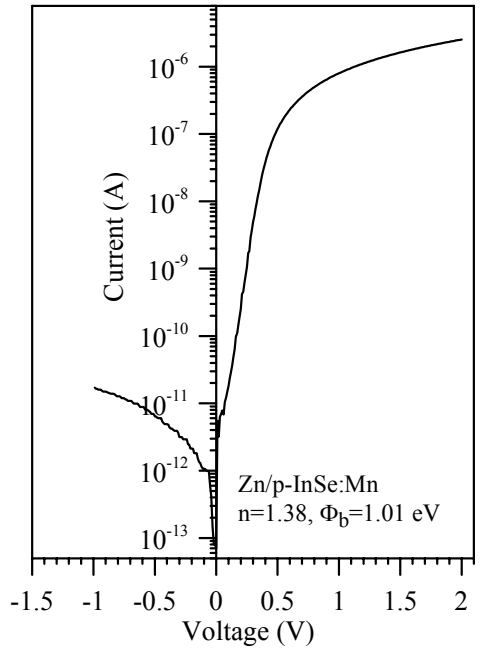

Fig. 12. Forward- and reverse-bias ln(I)–V characteristics of the Zn/p-InSe:Mn Schottky barrier diode at room temperature.

Table 1. The parameters obtained for all of the metal/p-InSe:Mn Schottky barrier diodes

Diodes	***n***	Φ_{b0} **(eV)**
Ag/*p*-InSe:Mn	1,41	0,93
Al/*p*-InSe:Mn	1,32	0,93
Au/*p*-InSe:Mn	1,49	0,93
Au-Be/*p*-InSe:Mn	1,19	0,91
Au-Ge/*p*-InSe:Mn	1,52	0,97
Au-Zn/*p*-InSe:Mn	1,15	0,94
Cd/*p*-InSe:Mn	1,19	0,82
Co/*p*-InSe:Mn	1,51	0,75
Mn/*p*-InSe:Mn	1,19	0,84
Sb/*p*-InSe:Mn	1,39	0,85
Sn/*p*-InSe:Mn	1,51	0,89
Zn/*p*-InSe:Mn	1,38	1,01

According to the thermionic emission theory, the forward bias ln (*I*)–*V* characteristics of a SBD with the series resistance can be expressed as [9]

$$I = I_0 \left[\frac{q(V - IR_S)}{nkT} \right] \tag{4}$$

where R_S is the series resistance and the IR_S term is the voltage drop across series resistance of device. The value of the series resistance can be determined from following functions using Eq. (1) for the data of downward curvature in the forward bias I–V characteristics. When $dV/d(\ln I)$ versus I is plotted using Eq. (5), this plot is a straight line region where dominates the series resistance.

$$\frac{dV}{d(\ln I)} = \frac{nkT}{q} + IR_S \tag{5}$$

A plot of $dV/d(\ln I)$ versus I should be linear and using Eq. (5), the slope and y-axis intercept of this plot will give R_S and nkT/q, respectively.

The values of the n and R_S are evaluated using the $H(I)$ functions developed by Cheung and Cheung [12], $H(I)$ are given as follows:

$$H(I) = V - \left(\frac{nkT}{q} \right) \ln \left(\frac{I}{AA^*T^2} \right) \tag{6}$$

and

$$H(I) = n\Phi_b + IR_S \tag{7}$$

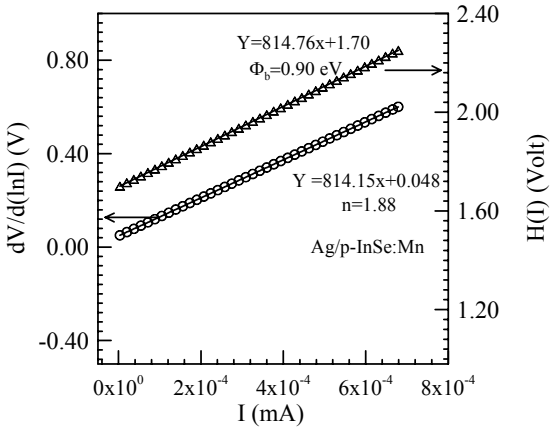

Fig. 13. A plot of $H(I)$ and $dV/d(\ln I)$ versus I obtained from forward bias current– voltage characteristics of the Ag/p-InSe:Mn Schotky barrier diodes at room temperature.

According to Eq. (7), a plot of $H(I)$ versus I should be linear. The slope of this plot provides a second determination of R_S and the value of the Φ_b can be obtained from the y-axis intercept because intercept of this line equal to $n\Phi_b$. These plots given in Fig. 13 are drawn using the data of the downward concave curvature region in the forward bias *I–V* characteristics given in Figs. 1-12. The values of n and R_S were determined using the Eq. (5), and the values of Φ_b and R_S were determined using the Eq. (7), respectively. It is seen that there is an good agreement between the two values of the series resistance

obtained from two different equations. The series resistance (R_s) of device plays an important role on electrical characteristics. Especially it can arise from five different sources: (1) the contact made by the probe wire to the gate; (2) the back contact of semiconductor; (3) impurities in semiconductor; (4) the resistance of quasi-neutral bulk semiconductor and (5) non-uniform doping distribution in the semiconductor [13-15]. The values of n and Φ_b also agree well with those values obtained from the linear regions of the forward bias *I–V* plot. The R_S values obtained from the two methods are in agreement with each other due to the consistency of the Cheung functions [12]. The various parameters obtained from Cheung functions [12] at the room temperature using Eqs. (5) and (7) are given Table 2. The BH values for the metal/*p*-InSe:Mn SBDs have varied from 0.75 to 1.01 eV, and *n* values from 1.51 to 1.15.

Table 2.The various parameters obtained from Cheung functions [12] at the room temperature

Diodes	n	Φ_b (eV)	R_S (kΩ) (From d*V*/d(ln*I*)-*I*)	R_S (kΩ) (From H(*I*)-*I*)
Ag/*p*-InSe:Mn	1,88	0,90	814,15	814,76
Al/*p*-InSe:Mn	1,80	0,90	138,84	140,12
Au/*p*-InSe:Mn	2,11	0,90	515,64	508,68
Au-Be/*p*-InSe:Mn	2,08	0,87	440,60	445,71
Au-Ge/*p*-InSe:Mn	2,11	0,91	632,43	609,23
Au-Zn/*p*-InSe:Mn	2,66	0,84	383,84	378,59
Cd/*p*-InSe:Mn	1,96	0,79	69,19	68,96
Co/*p*-InSe:Mn	1,96	0,74	184,96	185,40
Mn/*p*-InSe:Mn	1,96	0,78	168,47	169,26
Sb/*p*-InSe:Mn	2,35	0,83	398,81	409,89
Sn/*p*-InSe:Mn	2,11	0,82	399,29	402,58
Zn/*p*-InSe:Mn	2,00	0,93	583,88	564,03

4. Conclusions

The experimental *I-V* plots of the metals/p-InSe:Mn SBDs have been given in Figs. 1–12. Metal/*p*-InSe:Mn SBDs have showed rectifying behaviour. These structures obtained by applying easy processing steps. Due to rectifying properties, it is expected that InSe is an candidate for Schottky diodes. Various electrical parameters, such as ideality factor, BH, have been obtained using *I–V* characteristics. The BH values obtained from the I–V characteristics have varied between 0.75 eV and 1.01 eV with values of ideality factors ranging between 1.51 and 1.15 for the metal/p-InSe:Mn SBDs.

References

[1] A. Segura, J.P. Guesdon, J.M. Besson, A. Hevy, J. Appl. Phys. **54**, 876 (1983) .
[2] Z.D. Kovalyuk, V.M. Katerynchuk, A.I. Savchuk, .M. Sydor, Mater. Sci. Eng. B **109**, 252 (2004).
[3] S. Duman, B. Gurbulak, A. Turut, Appl. Surf. Sci. **253**, 3899 **(**2007).
[4] S. Duman, B. Gürbulak, S. Dogan, A. Turut, Microelectron. Eng. **86**, 106 (2009) .
[5] R. Mamy, X. Zaoui, J. Barrau and A. Chevy, Revue Phys. Appl. **25**, 947 (1990).
[6] K. Ando, A. Katsui, Thin Solid Films **76**, 141 (1981).
[7] S. Shigetomi, T. Ikari, J. Appl. Phys. **88**, 1520 (2000).
[8] C. Julien, E. Hatzikraniotis, A. Chevy, K. Kambas, Mater. Res. Bull. **20**, 287 (1985).
[9] E.H. Rhoderick, R.H. Williams, Metal-Semiconductor Contacts, second ed., Clarendon, Oxford (1988).
[10] S.M. Sze, Physics of Semiconductor Devices, second ed., Wiley, New York (1981)
[11] R.T. Tung, Mater. Sci. Eng. **235**, 1 (2001) .
[12] S.K. Cheung, N.W. Cheung, Appl. Phys. Lett. **49**, 85 (1986).
[13] H. Kanbur, S. Altindal, T. Mammadov, Y. Safak, J. Optoelectron. Adv. Mater. **13**, 713 (2011).
[14] D, Korucu, T.S. Mammadov, J. Optoelectron. Adv. Mater. **14**, 41 (2012).
[15] I. Kaya, A.Tataroglu, J. Optoelectron. Adv. Mater. **14,** 49 (2012).

*Corresponding author: sduman@atauni.edu.tr